ORIGINAL PAPER

MR imaging perfusion and diffusion analysis to assess preoperative Short Course Radiotherapy response in locally advanced rectal cancer: Standardized Index of Shape by DCE-MRI and intravoxel incoherent motion-derived parameters by DW-MRI

Antonella Petrillo[1] · Roberta Fusco[1] · Vincenza Granata[1] · Sergio Venanzio Setola[1] · Mario Sansone[2] · Daniela Rega[3] · Paolo Delrio[3] · Francesco Bianco[3] · Giovanni Maria Romano[3] · Fabiana Tatangelo[4] · Antonio Avallone[5] · Biagio Pecori[6]

Abstract

Our aim is to assess preoperative Short Course Radiotherapy (SCR) tumor response in locally advanced rectal cancer (LARC) through Standardized Index of Shape (SIS) by DCE-MRI, apparent diffusion coefficient (ADC) and intravoxel incoherent motion-derived parameters by DW-MRI. 35 patients with LARC underwent MR scan before and after SCR followed by delayed surgery, retrospectively, were enrolled. SIS, ADC, tissue diffusion (D_t), pseudodiffusion (D_p), and perfusion fraction (f) were extracted by MRI for each patient before and after SCR. Tumor regression grade (TRG) was estimated. Receiver operating characteristic curve and linear classification were performed. Sixteen patients were classified as responders (TRG $\leq$ 2) and 19 as non-responders. Seven patients had TRG1 [pathological complete response (pCR)]. The best parameter to discriminate responders by non-responders was SIS (sensitivity 94%, specificity 84%, accuracy 89%, cutoff value = − 7.8%). SIS obtained the best diagnostic performance also to discriminate pCR (sensitivity 86%, specificity 89%, accuracy 89%, cutoff value = 68.2%). No accuracy increase was obtained combining linearly each possible parameters couple or all functional MR-derived parameters. SIS is a hopeful DCE-MRI angiogenic biomarker to assess preoperative treatment response after SCR with delayed surgery, and it permits to discriminate pCR allowing to direct surgery for tailored and conservative treatment.

Keywords Rectal cancer · Radiotherapy · Perfusion magnetic resonance imaging · Diffusion magnetic resonance imaging · Diagnostic imaging

✉ Roberta Fusco
r.fusco@istitutotumori.na.it

1   Radiology Unit, Istituto Nazionale Tumori - IRCCS - Fondazione G. Pascale, Via Mariano Semmola, 80131 Naples, Italy

2   Department of Electrical Engineering and Information Technologies, University "Federico II" of Naples, Via Claudio, Naples, Italy

3   Gastrointestinal Surgical Oncology Unit, Istituto Nazionale Tumori - IRCCS - Fondazione G. Pascale, Via Mariano Semmola, 80131 Naples, Italy

4   Diagnostic Pathology Unit, Istituto Nazionale Tumori - IRCCS - Fondazione G. Pascale, Via Mariano Semmola, 80131 Naples, Italy

5   Gastrointestinal Medical Oncology Unit, Istituto Nazionale Tumori - IRCCS - Fondazione G. Pascale, Via Mariano Semmola, 80131 Naples, Italy

6   Radiotherapy Unit, Istituto Nazionale Tumori - IRCCS - Fondazione G. Pascale, Via Mariano Semmola, 80131 Naples, Italy

Introduction

Total mesorectal excision combined with preoperative radiation therapy and concomitant chemotherapy (CRT) is the current standard for locally advanced rectal cancer (LARC) [1–3]. Long-course CRT has been extensively applied, and encouraging results derive from this approach in terms of local control with a high percentage of tumor regression up to a significant rate of complete response [1–3]. However, Short Course Radiotherapy (SCR) is known to be a valuable therapeutic option in patients with LARC. A recent meta-analysis [4] reported that SCR with immediate surgery is as effective as long CRT with deferred surgery in terms of overall and disease-free survival rates, local and distant control, and toxicity. Also, Short Course Radiotherapy with Delayed Surgery (SCRDS) (after 4–8 weeks), optional therapy described for patients with locally advanced tumors who are not fit for CRT, leads to similar results in terms of negative margin resection percentage and satisfactory results about the downstaging and pathological response rate compared to traditional preoperative CRT [5–7]. Therefore, SCRDS can be considered effective in LARC downsizing, ensuring a significant pathological response rate [7–9], and can be considered an optional therapy in patients with locally advanced cancers who are not fit for CRT [10–13].

The use of new imaging modalities to make individual assessments of therapy response could be of great clinical value to adjust subsequent strategies tailored for each patient. Such strategies range from a tailored surgical approach to administering an adjuvant regimen, or even to a wait-and-see policy without surgery for patients with high surgical risks [14, 15].

Morphological MRI evaluation is the best imaging tool for locoregional LARC staging, consenting an accurate assessment of the disease extension, of the mesorectal fascia and lymph node involvement [16]. However, there are some restrictions: a positive tumor response cannot correspond to a significant tumor size reduction; there is difficulty to differentiate necrosis, fibrotic tissue, and viable residual tumor tissue within treated areas [16, 17]. Therefore, several studies focused their attention on the potential added benefit of functional quantitative parameters derived by MR image [17–20]. Combining functional information with anatomic detail provided by MRI, this imaging technique makes an actually powerful response assessment tool. Dynamic contrast-enhanced MRI (DCE-MRI) has demonstrated promising to detect residual tumor after pre-surgery CRT [17–21]. Previous studies have been investigated functional parameters derived by DCE-MRI data in rectal cancer [18–21] such as the Standardized Index of Shape proposed by Petrillo et al. [18] as a simple

semiquantitative parameter capable of differentiating pathological significant and complete response after CRT in LARC. Moreover, in various oncology fields, researchers have recommended the use of diffusion-weighted imaging (DWI) to assess treatment response [22–29]. DWI provides functional information on the tissues microstructure by means of the evaluation of water proton mobility differences [22, 23]. Water diffusion characteristics depend on cell density, vascularity, and viscosity of the extracellular fluid and cell membrane integrity. By quantifying these properties by means of the individual apparent diffusion coefficient (ADC) using mono-exponential model to analyze DWI data, it can be used as an imaging biomarker to reflect biological tumor changes and to monitor and predict treatment response [24, 25]. Moreover, using a by-exponential model to analyze DWI data, information on both diffusion and perfusion tissue properties derived from intravoxel incoherent motion method (IVIM) can be obtained: the pure tissue coefficient (D_t) that describes water macroscopic motion in the cellular interstitial space, the pseudodiffusion coefficient (D_p) that describes blood microscopic motion in the vessels, and the perfusion fraction (f) that describes the proportion of two different motions [26–29].

DCE-MRI and DW-MRI after CRT were shown to be more valuable than morphologic MR imaging to detect pathological significant and complete response, because on DCE and DW images, viable residual tumors are more easily recognized, as they appear hyperintense compared with the low signal intensity (SI) of the surrounding non-neoplastic tissue.

Aim of this study is to determine the diagnostic performance of MR imaging for the assessment of tumor response after SCRDS in patients with LARC using Standardized Index of Shape (SIS) obtained by DCE-MRI and using ADC and IVIM-derived parameters obtained by DW-MRI. Linear combination of each possible parameters couple and of all functional MR-derived parameters extracted by DCE- and DW-MRI was also evaluated.

Materials and methods

Patient selection

Thirty-five patients with a median age of 67 years (range 48–83 years) who refused or were considered unfit for chemoradiation and planned for neoadjuvant Short Course Radiotherapy were evaluated in this retrospective study, from May 2011 to December 2016.

Patient characteristics are described in Table 1.

All patients had a biopsy-proven rectal adenocarcinoma. Endorectal ultrasonography, MRI of pelvis, and Computed

Table 1 Patient characteristics and histopathological Findings

Characteristics	All patients $n = 35$ (%)	TRG 1–2 $n = 16$	TRG 3–4 $n = 19$	$p*$
Gender				> 0.05
Male/female	27 (77) 8 (23)	11/5	16/3	
Median age (range)	67 (48–83)	69 (48–78)	68 (48–76)	
Gunderson risk				> 0.05
Intermediate: T3N0, T2N1	8 (22.9)	3	5	
Moderately high: T2N2, T3N1, T4N0	18 (51.4)	8	10	
High: T3N2	9 (25.7)	5	4	
Distance from the anal verge				> 0.05
≤ 5 cm	14 (40.0)	6	8	
> 5 cm	21 (60.0)	10	11	
Circumferential resection margin				> 0.05
> 2 mm	16 (45.7)	7	9	
≤ 2 mm	13 (37.1)	6	7	
≤ 1 mm	5 (14.3)	2	3	
Not measurable	1 (2.9)	0	1	

Tomography (CT) scan of chest, abdomen, and pelvis were used as staging examinations. Patients had T2–T4 rectal cancer with or without local lymph node involvement. Patients staged T2 without lymph node involvement were included only if the tumor was located at less than 5 cm from the anal verge. Exclusion criteria were: inability to give informed consent, previous rectal surgery, and contraindications to MRI or to MR contrast media administration. Patients were included in the study in accordance with the approved guidelines of the local ethical committee of National Cancer Institute of Naples "Pascale Foundation" and gave their written informed consent.

Radiotherapy

All patients underwent dose-planning CT in prone position. After an online CT virtual simulation, CT datasets were transferred to a dedicated treatment planning system through a DICOM network and an individualized clinical target volume (CTV) was done, including the gross tumor volume with margins (2–3 cm depending upon tumor position, defined by MRI imaging), the mesorectum, and regional lymph nodes depending upon tumor location. We contoured the small bowel, the femoral heads, and the bladder as critical organs on all CT slices of every patient, and we evaluated the relative dose–volume histogram on the treatment planning console. Three-dimensional plans for 3D or intensity-modulated radiation therapy (IMRT) radiotherapy were generated for a dual-energy, 6–20 MV X-rays, (Clinac 2100, Varian Medical Systems, Palo Alto, CA) or 6–15 MV X-rays linear accelerator (Elekta Agility, Elekta Instrument AB Stockholm, Stockholm, Sweden) both equipped with multileaf collimators (MLC). Patients were scheduled using a three-field or IMRT treatment arrangement to include the planning target volume within the 95% isodose, and a dose of 25 Gy in five fractions over 1 week was prescribed to the ICRU 62 intersection point.

MRI data acquisitions

Each patient underwent MR studies before and after SCR: baseline, on average 23.8 days before starting radiotherapy and delayed, on average 61.0 days after the end of SCR. MR imaging was performed with a 1.5T scanner (Magnetom Symphony, Siemens Medical System, Erlangen, Germany) equipped with a phased-array body coil. Patients were placed in a supine, head-first position. Mild rectal lumen distension was achieved with 60–90 mL of non-diluted ferumoxil (Lumirem, Guerbet, RoissyCdGCedex, France) suspension introduced per rectum. Pre-contrast coronal T1w 2D turbo spin-echo (TSE) images and sagittal and axial T2w 2D turbo spin-echo images of the pelvis were obtained. Axial DWIs were acquired (spin-echo diffusion-weighted echo-planar imaging (SE-DW-EPI)) at seven b-values of 0, 50, 100, 150, 300, 600, 800 s/mm^2. Subsequently, axial, dynamic, contrast-enhanced T1w, FLASH 3D gradient-echo images were acquired. We obtained one sequence before and ten sequences, without any delay, after IV injection of 0.1 mmol/kg of a positive, gadolinium-based paramagnetic contrast medium (Gd-DOTA, Dotarem, Guerbet, Roissy-CdG-Cedex, France). The contrast medium was injected using Spectris Solaris® EP MR (MEDRAD Inc., Indianola, PA), with a flow rate of 2 mL/s, followed by a 10-mL saline flush at the same rate. Temporal resolution was 0.58 min, corresponding to 35 s (as reported in Table 2). Then, sagittal, axial, and coronal post-contrast T1w 2D turbo spin-echo images,

Table 2 Pulse Sequence Parameters on MR studies

Sequence	Orientation	TR/TE/FA (ms/ms/deg.)	AT (min)	FOV (mm × mm)	Acquisition matrix	ST/Gap (mm/mm)	TF
T1w 2D TSE	Coronal	499/13/150	2.36	450 × 450	256 × 230	3/0	3
T2w 2D TSE	Sagittal	4820/98/150	4.17	260 × 236	256 × 139	3/0	13
T2w 2D TSE	Axial	3970/98/150	3.48	270 × 236	256 × 157	3/0	13
SE-DW-EPI	Axial	2700/83	6.37	136 × 160	160 × 102	4/0	/
T1w FLASH 3D	Axial	9.8/4.76/25	0.58	330 × 247	256 × 192	3/0	/
T1w FLASH 3D	Axial	9.8/4.76/25	0.58 × 10	330 × 247	256 × 192	3/0	/
T1w 2D TSE	Sagittal	538/13/150	2.35	250 × 250	256 × 230	3/0	5
T1w 2D TSE	Coronal	538/13/150	2.52	250 × 250	256 × 230	3/0	5
T1w 2D TSE	Axial	450/12/150	2.31	270 × 236	256 × 202	3/0	5

TR repetition time, *TE* echo time, *FOV* field of view, *FA* flip angle, *ST* slice thickness, *TF* turbo factor, *AT* acquisition time

with and without fat saturation, were obtained (Table 2 Axial T1-w pre- and post-contrast sequences were acquired at the same position as the T2-w sequence. MRI total acquisition time was around 40 min. Each patient received bowel preparation and antispasmodic medication before any of the MR examinations in order to reduce respiratory artifacts.

MRI image data analysis

Images assessment was performed in a single reading session for each patient by consensus of two gastrointestinal radiologists with 20 and 8 years of experience in reading pelvic MR images.

To take into account tumor heterogeneity, the radiologists, based on pre-contrast T1-weighted images using the T2-weighted images as a guide [30], manually drew regions of interests (ROI) along contours of tumor to obtain volume of interest (VOI) for each study, covering the whole lesion with exclusion of peripheral fat, artefact, and blood vessels. After the treatment, the manually drawn regions of interests (ROI) include also the fibrosis induced by treatment, especially in the cases of pathological complete response. Median and standard deviation values were recorded for each VOI.

Median TIC of the segmented VOI was obtained and using that, the maximum signal difference (MSD) and washout slope (WOS) were calculated [31]. Then for SIS analysis, considering median value percentage change of MSD [$\Delta MSD = (MSD_1 - MSD_2)/MSD_1 \times 100$] and of WOS [$\Delta WOS = (WOS_1 - WOS_2)/WOS_1 \times 100$], their combination was evaluated as described in a previously paper [18].

Per each voxel on DW data was calculated ADC using mono-exponential model [22–25] while other diffusion and perfusion information (perfusion fraction f, pure tissue diffusion coefficient D_t, pseudodiffusion coefficient D_p) was obtained modeling DW-data using the IVIM model [26–29] and using variable projection algorithm for parameters

estimation [32]. An exhaustive description of the algorithm is beyond the scope of the present paper, and the interested reader is referred to [33]. Median values of ADC and IVIM-derived parameters of each VOI were obtained.

Per each MR descriptor, the percentage change between pre- and post-treatment was obtained as $\Delta X = (X\text{pre} - X\text{post})/X\text{pre}$ (X is the generic shape descriptor).

All analyses were performed using Matlab R2007a (The Math-Works Inc., Natick, MA).

Surgery

Surgery was performed on average 70.0 days after the end of radiotherapy. Based on the results of restaging and downsizing, sphincter-saving surgery was considered for all patients without a clear sphincter involvement before treatment, and local excision was considered for patients with a significant clinical response. The planned operation was discussed with the patients, and a specific informed consent was obtained. A rectal resection with total mesorectal excision and bilateral nerve sparing, when possible, was the standard approach. In distal cancers, an ultra-low anterior resection with colo-anal manual anastomosis or, in case of sphincter involvement, an abdomino-perineal resection was performed. All patients receiving an anastomosis underwent construction of a protecting ileostomy.

Evaluation of pathologic response

Details of how the pathologic response assessment was performed have been described [34, 35]. Briefly, surgical specimens containing the tumor were evaluated and scored according to tumor regression grade (TRG), as proposed by Mandard et al. [35] by an expert pathologist who was not aware of MRI findings. A score of TRG 1 means a complete response with absence of residual cancer and fibrosis

extending through the wall. TRG 2 is the presence of residual cancer cells scattered through the fibrosis. TRG 3 corresponds to an increased number of residual cancer cells, with predominant fibrosis. TRG 4 indicates residual cancer outgrowing fibrosis. TRG 5 is the absence of regressive changes. Patients with a TRG 1 or 2 score were considered as responders, whereas the remaining patients (TRG 3, 4, or 5) were classified as non-responders. Patients with TRG 1 were considered with pathological complete response while patients with TRG 2–5 were considered with incomplete pathological response [18].

Statistical analysis

All quantitative data values were expressed as medians ± standard deviation (SD). Tumor perfusion and diffusion percentage changes between responder and non-responder patients and between pathological complete and incomplete response were analyzed using the Mann–Whitney test. Receiver operating characteristic (ROC) curves were also used to compare the diagnostic performance of SIS and diffusion parameters percentage change. Area under ROC curve (AUC) was calculated, and optimal thresholds were obtained maximizing the Youden index. Sensitivity, specificity, positive predictive value (PPV), negative predictive value (NPV), and accuracy were performed considering optimal cutoff values. Fisher exact tests were used to investigate whether results were statistically significant.

Moreover, a linear classifier was used to assess the diagnostic performance of each parameters couple combinations using percentage change of single parameter before and after treatment ($\Delta f \& \Delta D_p$, $\Delta f \& \Delta D_t$, $\Delta D_p \& \Delta D_t$, SIS&ΔADC, SIS&Δf, SIS&ΔD_t, SIS&D_p, ΔADC&Δf, ΔADC&ΔD_t, ΔADC&D_p) and of all extracted parameters obtaining the sensitivity, specificity, PPV, NPV, and accuracy.

McNemar test was performed to evaluate difference in diagnostic performance of SIS versus DWI derived parameters performance.

A p value < 0.05 was considered significant for all tests. All analyses were performed using Statistics Toolbox of Matlab R2007a (The Math-Works Inc., Natick, MA).

Results

All patients in our series had rectal adenocarcinomas. Three patients were pathologically classified as T0, six as T1, 21 as T2, and five as T3. There were seven patients with a TRG 1, nine with a TRG 2, 11 with a TRG 3, eight with a TRG 4, and none with a TRG 5. Therefore, 16 patients were classified as responders, 19 as not responders, and seven patients as complete responders by TRG.

Mann–Whitney test showed statistically significant differences exclusively for SIS percentage change median values between responder and non-responder patients and between complete and incomplete pathological response (p value $\ll 0.001$). Median values for SIS and DWI derived parameters percentage change for responder and non-responder patients based on TRG were reported in Table 3. Table 4 shows performance of SIS change and diffusion parameters change while Table 5 shows the performance of each parameters couple combinations ($\Delta f \& \Delta D_p$, $\Delta f \& \Delta D_t$, $\Delta D_p \& \Delta D_t$, SIS&ΔADC, SIS&Δf, SIS&ΔD_t, SIS&D_p, ΔADC&Δf, ΔADC&ΔD_t, ΔADC&D_p) to differentiate responders from non-responders group and to discriminate complete pathological response from incomplete pathological response. Results were statistically significant for each parameter alone and for each combination of two parameters (Fisher test $p < 0.01$). Diagnostic performance of SIS to assess preoperative SCR response was statistically significant compared to ΔADC, Δf, ΔD_t, and ΔD_p performances resulting in an increase of sensitivity and specificity ($p < 0.05$ at McNemar test). Couple combinations of parameters or linear combination of all MR-derived parameters did not increase the diagnostic performance compared to SIS for both discrimination analyses (responders versus non-responders and pathological complete response versus incomplete response). Linear combination of all MR-derived parameters obtained an accuracy of 86 and 83%, respectively, to discriminate responder patients and pathological complete response after SCR.

Figure 1a shows ROC analysis for SIS and DWI derived parameters change to discriminate responders from

Table 3 SIS change and diffusion parameters change median values for responder and non-responder group

	ΔADC (%)	Δf (%)	ΔD_p (%)	ΔD_t (%)	SIS (%)
Non-responders ($n = 16$)	23.40 ± 14.60	-17.58 ± 85.33	-18.89 ± 135.27	31.81 ± 29.60	-32.96 ± 53.49
Responders ($n = 19$)	35.40 ± 18.10	-20.90 ± 95.96	-29.28 ± 131.40	25.96 ± 138.35	86.82 ± 51.80
All	24.96 ± 16.64	-17.58 ± 16.64	-18.89 ± 89.09	31.16 ± 131.64	15.57 ± 78.20
p value	0.15	0.87	0.84	0.74	$\ll 0.001$

Results are expressed as median value ± SD

* Mann–Witney test

Table 4 Performance of SIS change and diffusion parameters change

	AUC	Sensitivity	Specificity	PPV	NPV	Accuracy	Cutoff
Performance to discriminate responders from non-responders group							
ΔADC	0.64	0.56	0.84	0.75	0.70	0.71	34.27
Δf	0.48	0.38	0.74	0.55	0.58	0.57	36.48
ΔD_p	0.52	0.50	0.63	0.53	0.60	0.57	− 10.93
ΔD_t	0.47	0.19	0.95	0.75	0.58	0.60	61.67
SIS	0.94	0.94	0.84	0.83	0.94	0.89	− 7.76
Performance to discriminate complete pathological response from incomplete response							
ΔADC	0.63	0.57	0.82	0.44	0.88	0.77	36.38
Δf	0.63	0.57	0.82	0.44	0.88	0.77	42.19
ΔDp	0.32	1.00	0.14	0.23	1.00	0.31	− 276.49
ΔD_t	0.55	0.43	0.96	0.75	0.87	0.86	61.67
SIS	0.88	0.86	0.89	0.67	0.96	0.89	68.22

AUC area under curve, *PPV* positive predictive value, *NPV* negative predictive value

Table 5 Performance of combinations of SIS with the diffusion parameters change

	Sensitivity	Specificity	PPV	NPV	Accuracy
Performance to discriminate responders from non-responders group					
SIS&ΔADC	0.94	0.84	0.83	0.94	0.89
SIS&Δf	0.88	0.84	0.82	0.89	0.86
SIS&ΔD_p	0.88	0.84	0.82	0.89	0.86
SIS&ΔD_t	0.81	0.89	0.87	0.85	0.86
ΔD_p&Δf	0.44	0.63	0.50	0.57	0.54
ΔD_t&Δf	0.38	0.68	0.50	0.57	0.54
ΔD_t&ΔD_p	0.44	0.79	0.64	0.63	0.63
ΔADC&Δf	0.63	0.63	0.59	0.67	0.63
ΔADC&ΔD_p	0.63	0.63	0.59	0.67	0.63
ΔADC&ΔD_t	0.63	0.74	0.67	0.70	0.69
All parameters	0.88	0.84	0.82	0.89	0.86
Performance to discriminate complete pathological response from incomplete response					
SIS&ΔADC	0.86	0.75	0.46	0.95	0.77
SIS&Δf	0.86	0.82	0.55	0.96	0.83
SIS&ΔD_p	0.86	0.82	0.55	0.96	0.83
SIS&ΔD_t	0.86	0.79	0.50	0.96	0.80
ΔD_p&Δf	0.71	0.68	0.36	0.90	0.69
ΔD_t&Δf	0.43	0.68	0.25	0.83	0.63
ΔD_t&ΔD_p	0.43	0.79	0.33	0.85	0.71
ΔADC&Δf	0.43	0.64	0.23	0.82	0.60
ΔADC&ΔD_p	0.57	0.71	0.33	0.87	0.69
ΔADC&ΔD_t	0.57	0.75	0.36	0.88	0.71
All parameters	0.71	0.86	0.56	0.92	0.83

non-responders while Fig. 1b shows ROC analysis for SIS and diffusion parameters change to detect complete pathological response versus incomplete pathological response.

We reported representative MR images for responder and non-responder patients exclusively for SIS and ΔADC because these were the only quantitative MR parameters with high diagnostic accuracy to assess SCR response. Figures 2 and 3 show DCE-MRI images and SIS analysis for a responder and a non-responder patient: TRG = 1 and SIS = 70% and TRG = 4 and SIS = − 31%, respectively. Figures 4 and 5 show DW-MRI images and ADC map for a responder and a non-responder patient (TRG = 2 and TRG = 3, respectively).

Discussion and conclusions

In recent years, there has been growing interest in functional imaging modalities to increase diagnostic accuracy for therapy response assessment. These imaging modalities reflect the microstructural and metabolic properties of the tumor, allowing the evaluation of treatment-induced changes before morphological changes become apparent. DCE-MRI and DWI have emerged as powerful tools to predict and assess neoadjuvant therapy response for rectal cancer. In fact, DCE-MRI and DW-MRI after preoperative CRT were shown to be more valuable than morphologic MR imaging to recognize pathological significant and complete response and to discriminate viable residual tumor.

Objective of this study is to determine the diagnostic performance of DCE and DW imaging for the assessment of tumor response after SCRDS in patients with LARC using Standardized Index of Shape obtained by DCE-MRI and using ADC and intravoxel incoherent motion-derived parameters obtained by DW-MRI and their combinations. To the best of our knowledge, there are no studies in literature focused on comparison of DCE-MRI and DWI and their combination in locally advanced rectal cancer after SCRDS.

There are many studies that evaluate the single modality, DCE and DWI, in preoperative long CRT assessment [18–21, 36–38]. In our previously studies [18], we
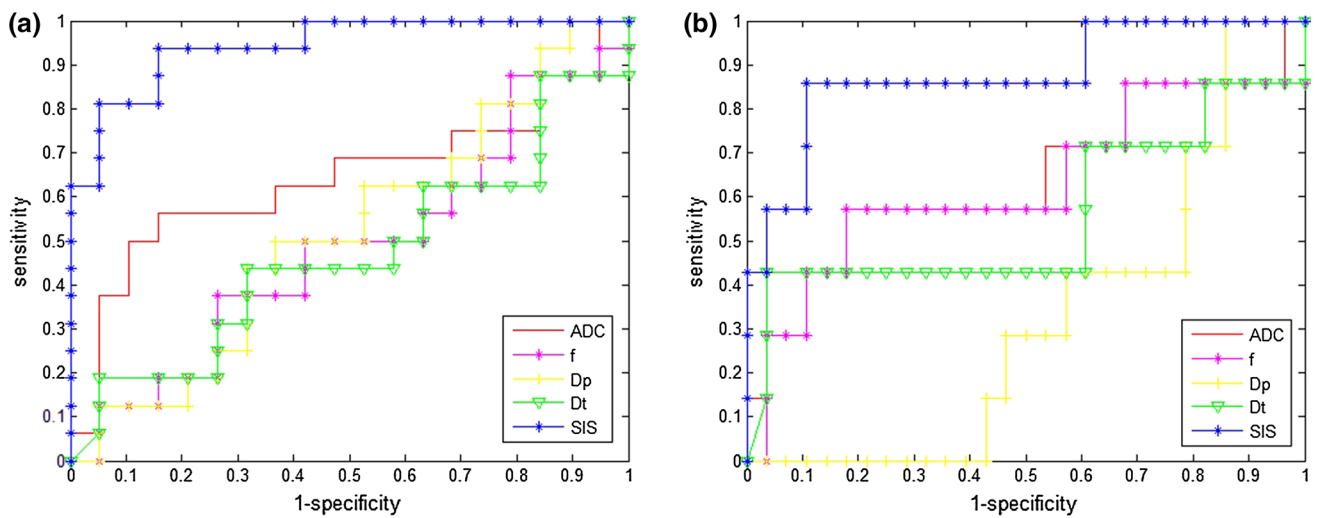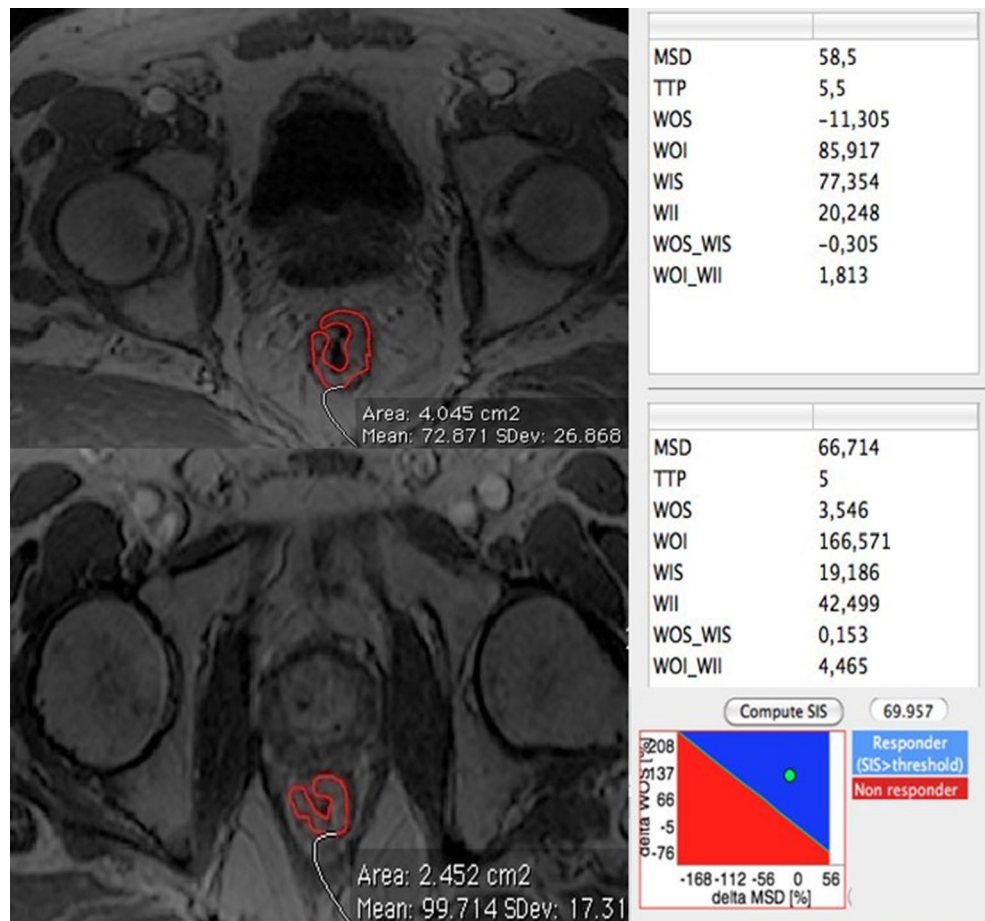
Fig. 1 ROC analysis for SIS and diffusion parameters by Varpro in discriminating responders from non-responders (**a**) and in discriminating complete pathological response from incomplete pathological response (**b**)
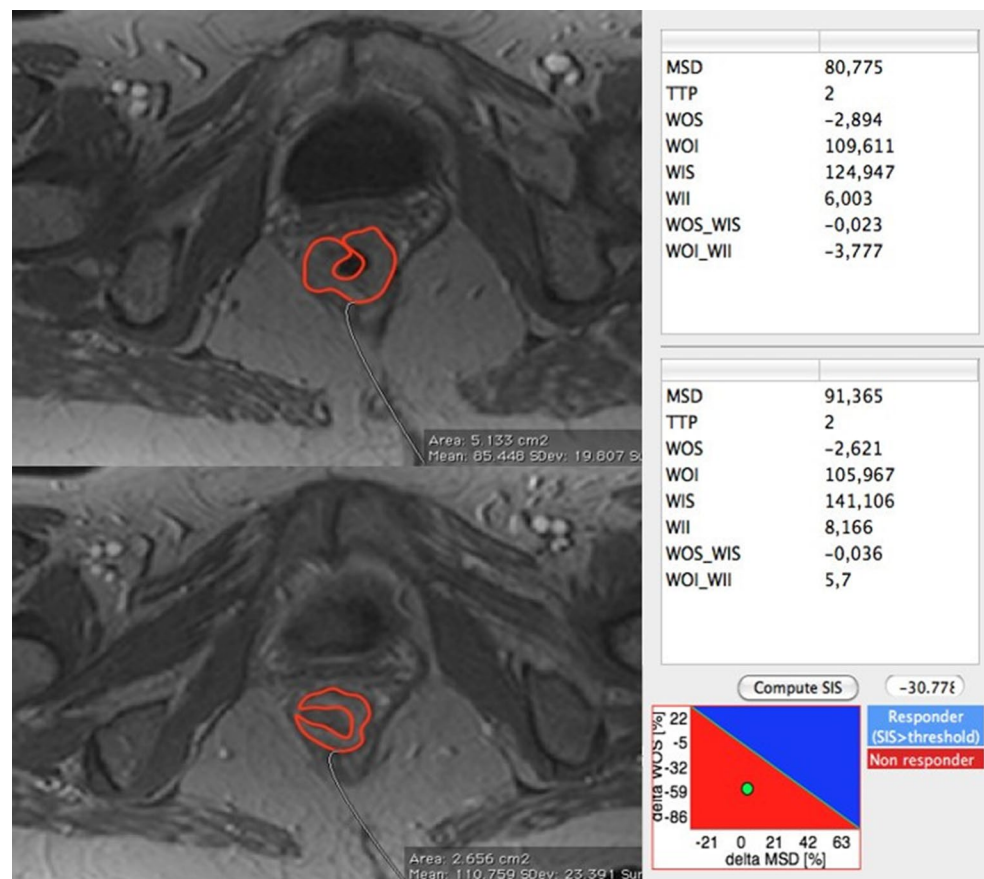

Fig. 2 DCE-MRI images and SIS analysis for a responder pre- (**a**–**c**) and post-treatment (**d**–**f**): TRG = 2 and SIS = 70%

demonstrated the ability of DCE-MRI using the Standardized Index of Shape to discriminate responder patients from non-responder patients and pathological complete tumor response after CRT in LARC with a good accuracy also when compared to FDG-PET examination [39]. Several studies demonstrated the role of diffusion-weighted

Fig. 3 DCE-MRI images and SIS analysis for a non-responder pre- (**a–c**) and post-treatment (**d–f**): TRG = 4 and SIS = − 31%

MSD	80,775
TTP	2
WOS	−2,894
WOI	109,611
WIS	124,947
WII	6,003
WOS_WIS	−0,023
WOI_WII	−3,777

MSD	91,365
TTP	2
WOS	−2,621
WOI	105,967
WIS	141,106
WII	8,166
WOS_WIS	−0,036
WOI_WII	5,7

imaging in LARC for early and late assessment of therapy response [36–38], and several studies evaluated the use of IVIM to elaborate DW-data in different kind of tumors [26–29, 40]. Choi et al. [36] demonstrated that ADC values have significant difference between pathological complete response and non-pathological complete response groups, demonstrating the utility of the ADC value as a quantitative objective biomarker in rectal cancer. Moreover, there are some studies with the aim to assess tumor response after SCR using metabolic change evaluations by FDG-PET with contrasting results [41–44]. Two studies [43, 44] have analyzed the responses to SCR in LARC, documenting no significant metabolic responses to SCR, while Pecori et al. [42] demonstrated that in the course of SCR, it is possible to estimate the probabilities of pathological tumor responses on the basis of logistic regression analysis of PET/CT parameters derived from three sequential studies.

Our findings showed that on the basis of only two MRI studies (basal and preparatory), there were statistically significant differences in SIS values between responders and non-responder patients and between complete and incomplete pathological response ($p \ll 0.01$ at Mann–Whitney test) while for ADC and IVIM-derived parameters percentage change, there were no statistically significant differences. The best parameters to discriminate responder patients from

non-responder patients by ROC analysis were SIS with a sensitivity of 94%, a specificity of 84%, and an accuracy of 89% using a cutoff value of − 7.8%. SIS obtained the best diagnostic performance also to differentiate complete complete pathological response from incomplete pathological response with a sensitivity of 86%, a specificity of 89%, and an accuracy of 89% using a cutoff value of 68.2%. Diagnostic performance of SIS to assess preoperative SCR response was statistically significant compared to ΔADC, Δf, ΔD_t, and ΔD_p performances, resulting in an increase of sensitivity and specificity ($p < 0.05$ at McNemar test). However, also, ΔADC showed a good diagnostic accuracy of 71.0% with a sensitivity of 56.0% and a specificity of 84.0% in discrimination of responders by non-responders and an accuracy of 77% with a sensitivity of 57.0% and a specificity of 82.0% to differentiate complete pathological response from incomplete pathological response after SCR. Moreover, also the pure diffusion coefficient (D_t) derived by IVIM analysis showed an high accuracy (86%) to discriminate complete pathological response from incomplete pathological response. Instead, couple combinations of parameters or linear combination of all MR-derived parameters did not increase the diagnostic performance compared to SIS for both discrimination analyses (responders versus non-responders and pathological complete response versus
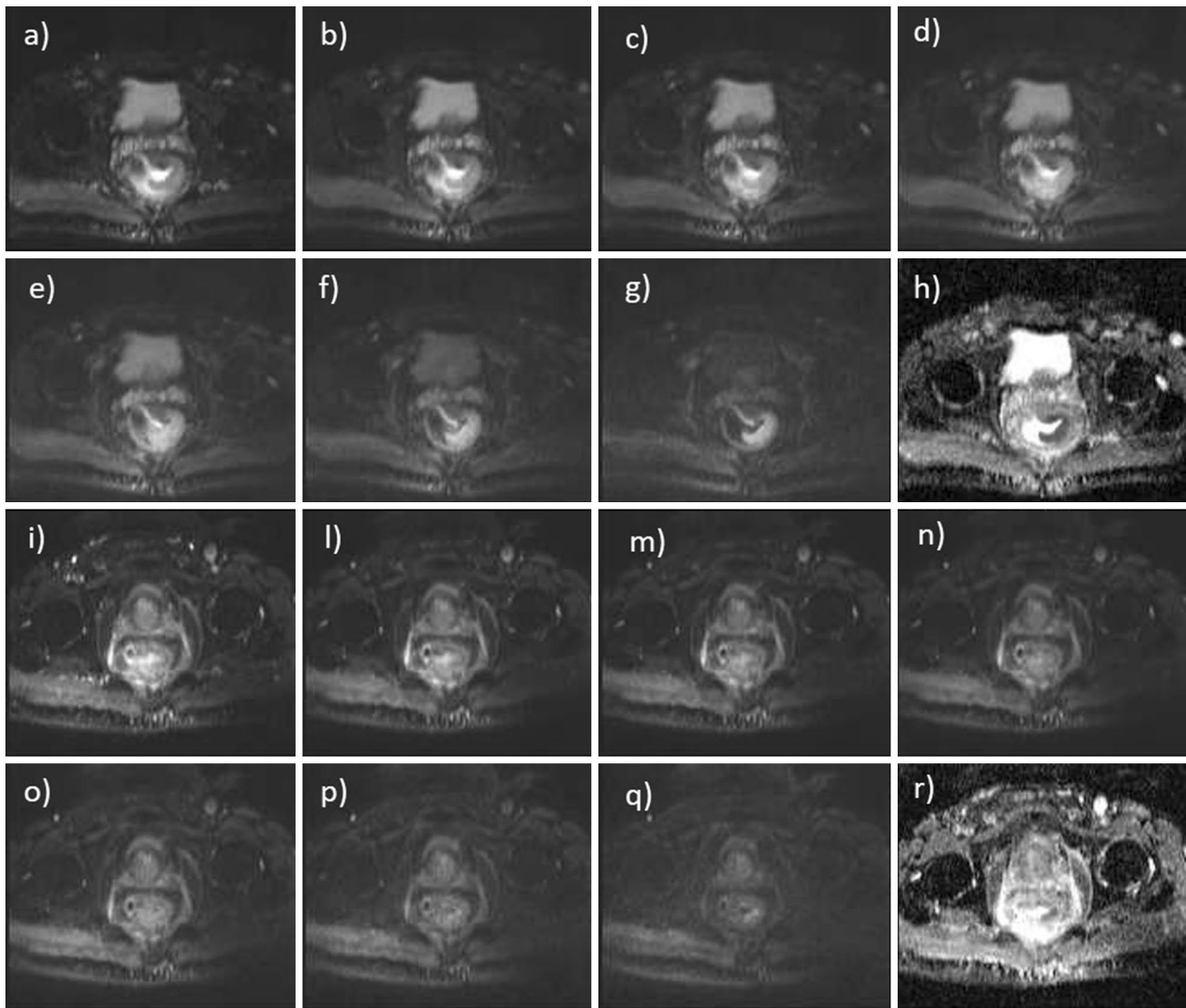
Fig. 4 DW-MRI images and ADC map for a responder pre (**a–h**) and post-treatment (**i–r**): TRG = 2 and ΔADC = 36%

incomplete response). Our results are comparable to those reported in recent literature such as the findings of Nougaret et al. [38]; these demonstrated that ADC values obtained after long CRT were useful for discrimination between good and poor responders. However, the Standardized Index of Shape, a simple quantitative parameters representative of tissue vascularization, showed the best results to assess tumor response after SCR.

Further studies are necessary to evaluate whether the combination of different functional imaging techniques may increase the specificity therapy response after SCR as already demonstrated by Lambrecht et al. [45] with the combination of 18F-FDG PET/CT with pre-treatment DWI to increase the specificity of response assessment. However, our results in SCRDS showed that combining SIS and diffusion parameters using a linear classifier no improvement of

diagnostic performance was obtained respect to SIS alone. SIS alone, with a simple formulas, allows to accurately assess the SCR response prior to surgery.

Some potential limitations deserve a special consideration: Two radiologists evaluated the MR images by consensus and in a single session per patient so that the intra-observer variability was not assessed. A more extensive patient panel would probably strengthen the power of SIS in SCR therapy assessment. A reproducibility analysis of IVIM-derived parameters was not performed; however, the use of median values for each DCE- and DW parameters extracted by volume of interest allows obtaining more robust measures.

In conclusion, the Standardized Index of Shape is a hopeful DCE-MRI angiogenic biomarker to assess pre-operative treatment response after SCR with delayed
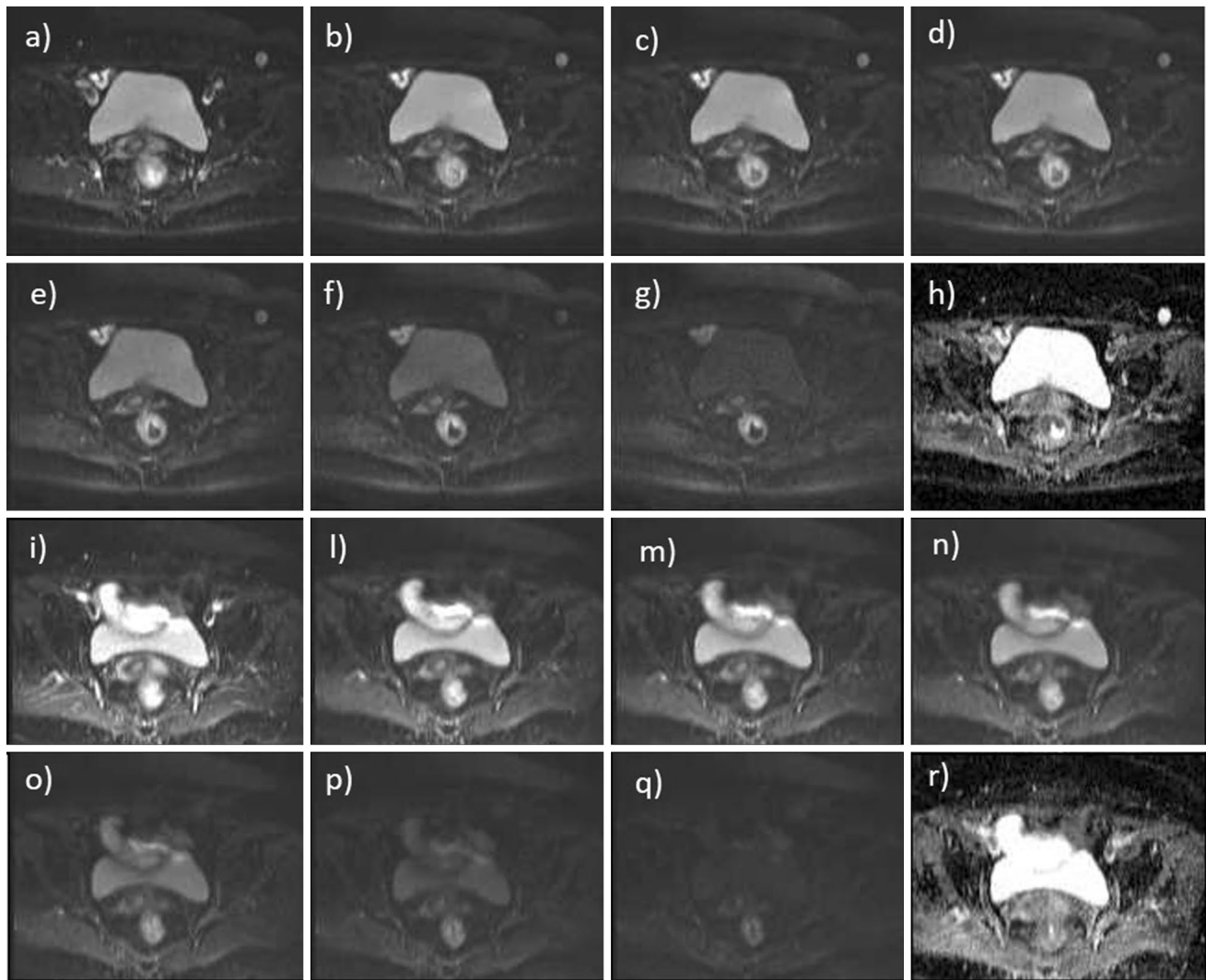
Fig. 5 DW-MRI images and ADC map for a non-responder pre- (**a**–**h**) and post-treatment (**i**–**r**): TRG = 4 and ΔADC = 8%

surgery, and it permits to discriminate pathological complete response allowing to direct surgery for tailored and conservative treatment.

Compliance with ethical standards

References

1. Avallone A, Aloj L, Delrio P, Pecori B, Leone A, Tatangelo F, Perri F, Petrillo A, Scott N, Budillon A. Multidisciplinary approach to rectal cancer: Are we ready for selective treatment strategies? Anticancer Agents Med Chem. 2013;13(6):852–60.
2. Avallone A, Delrio P, Guida C, Tatangelo F, Petrillo A, Marone P, Cascini LG, Morrica B, Lastoria S, Parisi V, Budillon A, Comella P. Biweekly oxaliplatin, raltitrexed, 5-fluorouracil and folinic acid

combination chemotherapy during preoperative radiation therapy for locally advanced rectal cancer: a phase I–II study. Br J Cancer. 2006;94(12):1809–15.

3. Delrio P, Avallone A, Guida C, Lastoria S, Tatangelo F, Cascini GM, Marone P, Petrillo A, Budillon A, Di Marzo M, Palaia R, Albino V, De Rosa V, Parisi V. Multidisciplinary approach to locally advanced rectal cancer: results of a single institution trial. Suppl Tumori. 2005;4(3):S8.

4. Zhou ZR, Liu SX, Zhang TS, Chen LX, Xia J, Hu ZD, Li B. Short-course preoperative radiotherapy with immediate surgery versus long-course chemoradiation with delayed surgery in the treatment of rectal cancer: a systematic review and meta-analysis. Surg Oncol. 2014;23(4):211–21.

5. Latkauskas T, Pauzas H, Gineikiene I, Janciauskiene R, Juozaityte E, Saladzinskas Z, et al. Initial results of a randomized controlled trial comparing clinical and pathological downstaging of rectal cancer after preoperative short-course radiotherapy or long-term chemoradiotherapy, both with delayed surgery. Colorectal Dis. 2012;14(3):294–8.

6. Bujko K, Kolodziejczyk M. The 5 × 5 Gy with delayed surgery in non-resectable rectal cancer: a new treatment option. Radiother Oncol. 2008;87(3):311–3.

7. Beppu N, Matsubara N, Noda M, Yamano T, Kakuno A, Doi H, Kamikonya N, Kimura F, Yamanaka N, Yanagi H, Tomita N. Short-course radiotherapy with delayed surgery versus conventional chemoradiotherapy: a comparison of the short- and long-term outcomes in patients with T3 rectal cancer. Surgery. 2015;158(1):225–35.

8. Pettersson D, Holm T, Iversen H, Blomqvist L, Glimelius B, Martling A. Preoperative short-course radiotherapy with delayed surgery in primary rectal cancer. Br J Surg. 2012;99(4):577–83.

9. Pettersson D, Lörinc E, Holm T, Iversen H, Cedermark B, Glimelius B, Martling A. Tumour regression in the randomized Stockholm III Trial of radiotherapy regimens for rectal cancer. Br J Surg. 2015;102(8):972–8 **discussion 8**.

10. Radu C, Berglund A, Pahlman L, Glimelius B. Short-course preoperative radiotherapy with delayed surgery in rectal cancer—a retrospective study. Radiother Oncol. 2008;87(3):343–9.

11. Hatfield P, Hingorani M, Radhakrishna G, Cooper R, Melcher A, Crellin A, Kwok-Williams M, Sebag-Montefiore D. Short-course radiotherapy, with elective delay prior to surgery, in patients with unresectable rectal cancer who have poor performance status or significant co-morbidity. Radiother Oncol. 2009;92(2):210–4.

12. Valentini V, Glimelius B, Haustermans K, Marijnen CA, Rodel C, Gambacorta MA, et al. EURECCA consensus conference highlights about rectal cancer clinical management: the radiation oncologist's expert review. Radiother Oncol. 2014;110(1):195–8.

13. Avallone A, Piccirillo MC, Delrio P, Pecori B, Di Gennaro E, Aloj L, Tatangelo F, D'Angelo V, Granata C, Cavalcanti E, Maurea N, Maiolino P, Bianco F, Montano M, Silvestro L, Terranova Barberio M, Roca MS, Di Maio M, Marone P, Botti G, Petrillo A, Daniele G, Lastoria S, Iaffaioli VR, Romano G, Caracò C, Muto P, Gallo C, Perrone F, Budillon A. Phase 1/2 study of valproic acid and short-course radiotherapy plus capecitabine as preoperative treatment in low-moderate risk rectal cancer-V-shoRT-R3 (Valproic acid–short Radiotherapy–rectum 3rd trial). BMC Cancer. 2014;24(14):875.

14. Heo SH, Kim JW, Shin SS, Jeong YY, Kang H-K. Multimodal imaging evaluation in staging of rectal cancer. World J Gastroenterol. 2014;20(15):4244–55.

15. Fusco R, Sansone M, Petrillo M, Avallone A, Delrio P, Tatangelo F, Petrillo A. Role of magnetic resonance imaging in locally advanced rectal cancer, colorectal cancer—surgery, diagnostics and treatment. In: Khan J, editor. InTech. 2014. https://doi.org/10.5772/56831.

16. Beets-Tan RG, Beets GL. Rectal cancer: review with emphasis on MR imaging. Radiology. 2004;232(2):335–46.

17. Leach MO, Brindle KM, Evelhoch JL, Griffiths JR, Horsman MR, Jackson A, Jayson GC, Judson IR, Knopp MV, Maxwell RJ, McIntyre D, Padhani AR, Price P, Rathbone R, Rustin GJ, Tofts PS, Tozer GM, Vennart W, Waterton JC, Williams SR, Workman P, Pharmacodynamic/Pharmacokinetic Technologies Advisory Committee, Drug Development Office, Cancer Research UK. The assessment of antiangiogenic and antivascular therapies in early-stage clinical trials using magnetic resonance imaging: issues and recommendations. Br J Cancer. 2005;92(9):1599–610.

18. Petrillo A, Fusco R, Petrillo M, Granata V, Sansone M, Avallone A, Delrio P, Pecori B, Tatangelo F, Ciliberto G. Standardized Index of Shape (SIS): a quantitative DCE-MRI parameter to discriminate responders by non-responders after neoadjuvant therapy in LARC. Eur Radiol. 2015;25(7):1935–45.

19. Petrillo M, Fusco R, Catalano O, Sansone M, Avallone A, Delrio P, Pecori B, Tatangelo F, Petrillo A. MRI for assessing response to neoadjuvant therapy in locally advanced rectal cancer using DCE-MR and DW-MR data sets: a preliminary report. Biomed Res Int. 2015;2015:514740.

20. Beets-Tan RG, Beets GL. MRI for assessing and predicting response to neoadjuvant treatment in rectal cancer. Nat Rev Gastroenterol Hepatol. 2014;11(8):480–8.

21. Phongkitkarun S, Tohmad U, Larbcharoensub N, Sumbunnanondha K, Swangsilpa T, Sirachainan E. DCE-MRI-derived parameters as predictors of response to neo-adjuvant chemoradiation treatment of rectal carcinoma. J Med Assoc Thai. 2016;99(3):338–47.

22. Le Bihan D, Breton E, Lallemand D, Aubin ML, Vignaud J, Laval-Jeantet M. Separation of diffusion and perfusion in intravoxel incoherent motion MR imaging. Radiology. 1988;168(2):497–505.

23. Le Bihan D, Breton E, Lallemand D, Grenier P, Cabanis E, Laval-Jeantet M. MR imaging of intravoxel incoherent motions: application to diffusion and perfusion in neurologic disorders. Radiology. 1986;161(2):401–7.

24. Oto A, Yang C, Kayhan A, Tretiakova M, Antic T, Schmid-Tannwald C, Eggener S, Karczmar GS, Stadler WM. Diffusion-weighted and dynamic contrast-enhanced MRI of prostate cancer: correlation of quantitative MR parameters with Gleason score and tumor angiogenesis. AJR Am J Roentgenol. 2011;197(6):1382–90.

25. Curvo-Semedo L, Lambregts DM, Maas M, Thywissen T, Mehsen RT, Lammering G, Beets GL, Caseiro-Alves F, Beets-Tan RG. Rectal cancer: assessment of complete response to preoperative combined radiation therapy with chemotherapy–conventional MR volumetry versus diffusion-weighted MR imaging. Radiology. 2011;260(3):734–43.

26. Deux AJ-F, Brugieres P, Rahmouni A. Liver cirrhosis: intravoxel incoherent motion MR imaging-pilot study. Radiology. 2008;249(3):891–9.

27. Wirestam R, Borg M, Brockstedt S, Lindgren A, Holtas S, Stahlberg F. Perfusion-related parameters in intravoxel incoherent motion MR imaging compared with CBV and CBF measured by dynamic susceptibility contrast MR technique. Acta Radiol. 2001;42(2):123–8.

28. Granata V, Fusco R, Catalano O, Guarino B, Granata F, Tatangelo F, Avallone A, Piccirillo M, Palaia R, Izzo F, Petrillo A. Intravoxel incoherent motion (IVIM) in diffusion-weighted imaging (DWI) for Hepatocellular carcinoma: correlation with histologic grade. Oncotarget. 2016;7(48):79357–64.

29. Granata V, Fusco R, Catalano O, Filice S, Amato DM, Nasti G, Avallone A, Izzo F, Petrillo A. Early assessment of colorectal cancer patients with liver metastases treated with antiangiogenic drugs: the role of intravoxel incoherent motion in diffusion-weighted imaging. PLoS ONE. 2015;10(11):e0142876.

30. Dresen RC, Beets GL, Rutten HJ, Engelen SM, Lahaye MJ, Vliegen RF, de Bruïne AP, Kessels AG, Lammering G, Beets-Tan RG. Locally advanced rectal cancer: MR imaging for restaging after neoadjuvant radiation therapy with concomitant chemotherapy. Part I. Are we able to predict tumor confined to the rectal wall? Radiology. 2009;252(1):81–91.

31. Fusco R, Petrillo A, Petrillo M, Sansone M. Use of tracer kinetic models for selection of semi-quantitative features for DCE-MRI data classification. Appl Magn Reson. 2013;44(11):1311–24.

32. Fusco R, Sansone M, Petrillo A. A comparison of fitting algorithms for diffusion-weighted MRI data analysis using an intravoxel incoherent motion model. MAGMA. 2017;30(2):113–20.

33. Seber GAF, Wild CJ. Nonlinear regression. New York: Wiley; 1989.

34. Andreola S, Leo E, Belli F, Bonfanti G, Sirizzotti G, Greco P, Valvo F, Tomasic G, Gallino GF. Adenocarcinoma of the lower third of the rectum surgically treated with a < 10-mm distal clearance: preliminary results in 35 N0 patients. Ann Surg Oncol. 2001;8(7):611–5.

35. Mandard AM, Dalibard F, Mandard JC, Marnay J, Henry-Amar M, Petiot JF, Roussel A, Jacob JH, Segol P, Samama G, et al. Pathologic assessment of tumor regression after preoperative chemoradiotherapy of esophageal carcinoma. Clinicopathologic correlations. Cancer. 1994;73(11):2680–6.

36. Choi MH, Oh SN, Rha SE, Choi JI, Lee SH, Jang HS, Kim JG, Grimm R, Son Y. Diffusion-weighted imaging: apparent diffusion coefficient histogram analysis for detecting pathologic complete response to chemoradiotherapy in locally advanced rectal cancer. J Magn Reson Imaging. 2015. https://doi.org/10.1002/jmri.25117.

37. Doi H, Beppu N, Kato T, Noda M, Yanagi H, Tomita N, Kamikonya N, Hirota S. Diffusion-weighted magnetic resonance imaging for prediction of tumor response to neoadjuvant chemoradiotherapy using irinotecan plus S-1 for rectal cancer. Mol Clin Oncol. 2015;3(5):1129–34.

38. Nougaret S, Vargas HA, Lakhman Y, Sudre R, Do RK, Bibeau F, Azria D, Assenat E, Molinari N, Pierredon MA, Rouanet P, Guiu B. Intravoxel incoherent motion-derived histogram metrics for assessment of response after combined chemotherapy and radiation therapy in rectal cancer: initial experience and comparison between single-section and volumetric analyses. Radiology. 2016;280(2):446–54.

39. Petrillo A, Fusco R, Petrillo M, Granata V, Delrio P, Bianco F, Pecori B, Botti G, Tatangelo F, Caracò C, Aloj L, Avallone A, Lastoria S. Standardized Index of Shape (DCE-MRI) and standardized uptake value (PET/CT): two quantitative approaches to discriminate chemo-radiotherapy locally advanced rectal cancer responders under a functional profile. Oncotarget. 2017;8(5):8143–53.

40. Iima M, Le Bihan D. Clinical intravoxel incoherent motion and diffusion mr imaging: past, present, and future. Radiology. 2016;278(1):13–32.

41. Rega D, Pecori B, Scala D, Avallone A, Pace U, Petrillo A, Aloj L, Tatangelo F, Delrio P. Evaluation of tumor response after short-course radiotherapy and delayed surgery for rectal cancer. PLoS ONE. 2016;11(8):e0160732.

42. Pecori B, Lastoria S, Caracò C, Celentani M, Tatangelo F, Avallone A, Rega D, De Palma G, Mormile M, Budillon A, Muto P, Bianco F, Aloj L, Petrillo A, Delrio P. Sequential PET/CT with [18F]-FDG predicts pathological tumor response to preoperative short course radiotherapy with delayed surgery in patients with locally advanced rectal cancer using logistic regression analysis. PLoS ONE. 2017;12(1):e0169462.

43. Siegel R, Dresel S, Koswig S, Gebauer B, Hunerbein M, Schneider W, Schlag PM. Response to preoperative short-course radiotherapy in locally advanced rectal cancer: value of f-fluorodeoxyglucose positron emission tomography. Onkologie. 2008;31(4):166–72.

44. Janssen MH, Ollers MC, van Stiphout RG, Buijsen J, van den Bogaard J, de Ruysscher D, Lambin P, Lammering G. Evaluation of early metabolic responses in rectal cancer during combined radiochemotherapy or radiotherapy alone: sequential FDG-PET-CT findings. Radiother Oncol. 2010;94(2):151–5.

45. Lambrecht M, Deroose C, Roels S, Vandecaveye V, Penninckx F, Sagaert X, van Cutsem E, de Keyzer F, Haustermans K. The use of FDG-PET/CT and diffusion weighted magnetic resonance imaging for response prediction before, during and after preoperative chemoradiotherapy for rectal cancer. Acta Oncol. 2010;49:956–63.